Available online at www.sciencedirect.com
ScienceDirect
Journal of the European Ceramic Society 28 (2008) 383–391
www.elsevier.com/locate/jeurceramsoc

Formation mechanism and microstructure development in acicular mullite ceramics fabricated by controlled decomposition of fluorotopaz

Aleksander J. Pyzik *, Clifford S. Todd, Chan Han

The Dow Chemical Company, Core R&D, Midland, MI 48764, USA

Available online 3 May 2007

Abstract

The Dow Chemical Company has developed a ceramic wall flow filter for use as a diesel particulate filter (DPF). It is composed of mullite grown from the low temperature (1000–1200 °C) decomposition of fluorotopaz in the presence of silicon tetrafluoride. Mullite grains are acicular (aspect ratio ~20), and their size can be controlled by raw material and processing variables (diameters chosen from 3 to 50 μm). The acicular mullite grains interlock forming an efficient filter with low back pressure. Heating precursors in air or introducing SiF_4 at temperature does not lead to a similar mullite microstructure. Characterization of samples quenched during the transformation from fluorotopaz to mullite indicates that growth of mullite was facilitated by a melt. The mullite formed is alumina-poor and chemically zoned from a molecular ratio $Al_2O_3/SiO_2 = 1.25$ in the core to $Al_2O_3/SiO_2 = 1.7$ in the rim. This mullite composition (5:4–7:4) appears to be stable across a broad range of temperatures.

Keywords: Grain growth; Powders-gas phase reaction; Mullite; Glass; Fluorotopaz

1. Introduction

Diesel engines have better fuel economy compared to gasoline engines due to their lean burn diffusion combustion plus the advantage of overall low emissions such as carbon monoxide (CO), hydrocarbons (HC), and nitrous oxide (NOx). However, further NOx reduction from diesel exhaust by after-treatment systems is extremely challenging. Therefore, most of the current NOx reduction on diesel engines is done through engine combustion processes, such as engine gas recirculation (EGR) and multiple fuel injections. The side effect of this approach is additional particulate matter (PM) or soot. Recent new regulations mandating very low levels of these emissions in Europe, North America, and Japan are the driving force behind the market demand for finding new technical solutions. Exhaust after-treatment is an essential component required for clean diesel technology. PM reduction in diesel exhaust is demanded for all the diesel engines that meet Euro V regulation. In general, a typical after-treatment system for PM control consists of a ceramic or metal porous filter that can capture soot or PM from diesel exhaust. A low-pressure drop and high soot capacity is desired. To meet these requirements, a wall flow filter with high porosity and a targeted specific pore size distribution (to assure low back pressure) is preferred. In addition, such a filter material should be stable at high temperature and have good chemical resistance to components such as ash, as well as high mechanical integrity to assure durability. Commercially available diesel particulate filters (DPF) are produced today from cordierite and silicon carbide. However, these materials produced from ceramic powder particles have severe limitations in the amount of porosity that can be incorporated into the honeycomb wall without excessively lowering their mechanical integrity or reducing the ability to filter nanosized particles.

The development of ceramic materials at The Dow Chemical Company has focused on technologies that produce highly porous materials with controllable grain and pore size distribution and high aspect ratio grains.[1–4] Mullite has been selected as a target material because of its ability to crystallize in the form of long needles and its well known stability at high temperature, high corrosion resistance, and high strength. The presence of mullite in sintered porcelain bodies has been known for a long time.[5] More recently Perera and Allot grew 0.5 μm wide and 5 μm long mullite needles by firing kaolinite between 1400 and 1600 °C.[6] Li et al.,[7] Hashimoto and Yamaguchi[8] and De Sousa

* Corresponding author.
E-mail address: apyzik@dow.com (A.J. Pyzik).

0955-2219/$ – see front matter © 2007 Elsevier Ltd. All rights reserved.
doi:10.1016/j.jeurceramsoc.2007.03.021

et al.[9] produced mullite needles from melts in flux-assisted processes but these needles typically were small and/or required temperatures well over 1300 °C (which also led to simultaneous densification). Other researchers used gas transport mechanisms to grow mullite based on the decomposition of volatile fluorine compounds. Okada and Otsuka[10] produced 9 μm long needles at 1600 °C, Choi and Li synthesized mullite needles several hundred microns long and about 1 μm wide from mixtures of silica and silicon in an alumina tube reactor under a flow of hydrogen and carbon tetrafluoride gas.[11] Miao[12] used natural fluorotopaz sand to produce mullite fibers with a diameter of less than 1 μm and length up to 10 μm. Unfortunately, all these methods led to materials consisting of small diameter mullite grains, typically with a small inter-grain pore size and, as a result, very high back pressure during filtration and regeneration.

Dow's approach is based on the formation of mullite during low temperature decomposition of fluorotopaz ($Al_2SiO_4F_2$).[2] In the first stage of this process fluorotopaz is formed from clay and Al_2O_3 in the presence of silicon tetrafluoride (SiF_4) gas. Upon subsequent heating, fluorotopaz decomposes endothermically to form mullite and SiF_4 gas at temperatures between 1000 and 1200 °C.[13] The unique feature of mullite resulting from controlled decomposition of fluorotopaz is a highly elongated (acicular) grain structure. The formation and growth of acicular mullite grains results in an interlocking microstructure with high porosity. This porosity remains virtually unchanged until 1400–1450 °C. In addition, the size of mullite crystals can be controlled depending on the raw materials and processing conditions. The typical aspect ratio remains about 20 but the overall grain size can be changed from diameters of about 3–50 μm. Therefore the microstructure can be tailored for DPF applications, where an average pore size between 15 and 20 μm in the honeycomb wall is advantageous.

The objective of this paper is to characterize the chemistry and growth mechanism of acicular mullite formed in Dow's process during controlled decomposition of fluorotopaz. Controlling the fluorotopaz decomposition process leads to a variety of mullite crystal and pore size distributions. This, in turn, allows for designing new DPFs that have enhanced filtration and regeneration characteristics.

2. Experimental

2.1. Raw materials and fabrication of acicular mullite ceramics

Acicular mullite can be made using many different sources of alumina and silica, but for the purpose of this work kaolinite clay and a high purity aluminum oxide powder were selected. The ratio of Al_2O_3/SiO_2 (wt.%) in the clay was 0.55 and the major impurities were as follows (in wt.%): Fe_2O_3, 1.6; TiO_2, 1.3; K_2O, 0.9; MgO, 0.6; CaO, 0.3.

Precursor honeycombs were made by combining the clay and alumina with processing additives such as water, binder, and lubricant. The resultant mix was extruded into 5.66 in. outside diameter × 6 in. length honeycombs. Honeycombs were

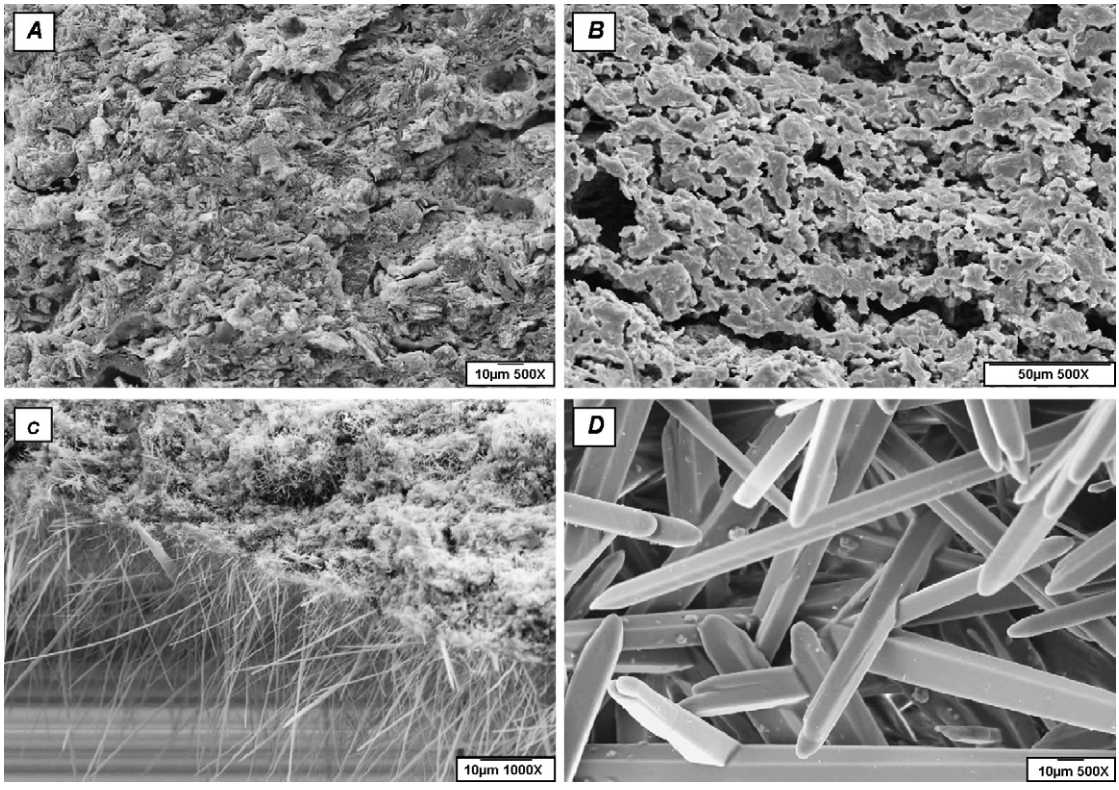

Fig. 1. SEM micrographs of mullite produced from the same precursor by three different routes: (A and B) by heating in air; (C) by heating in nitrogen, then introducing SiF_4; (D) by introducing SiF_4, then heating.

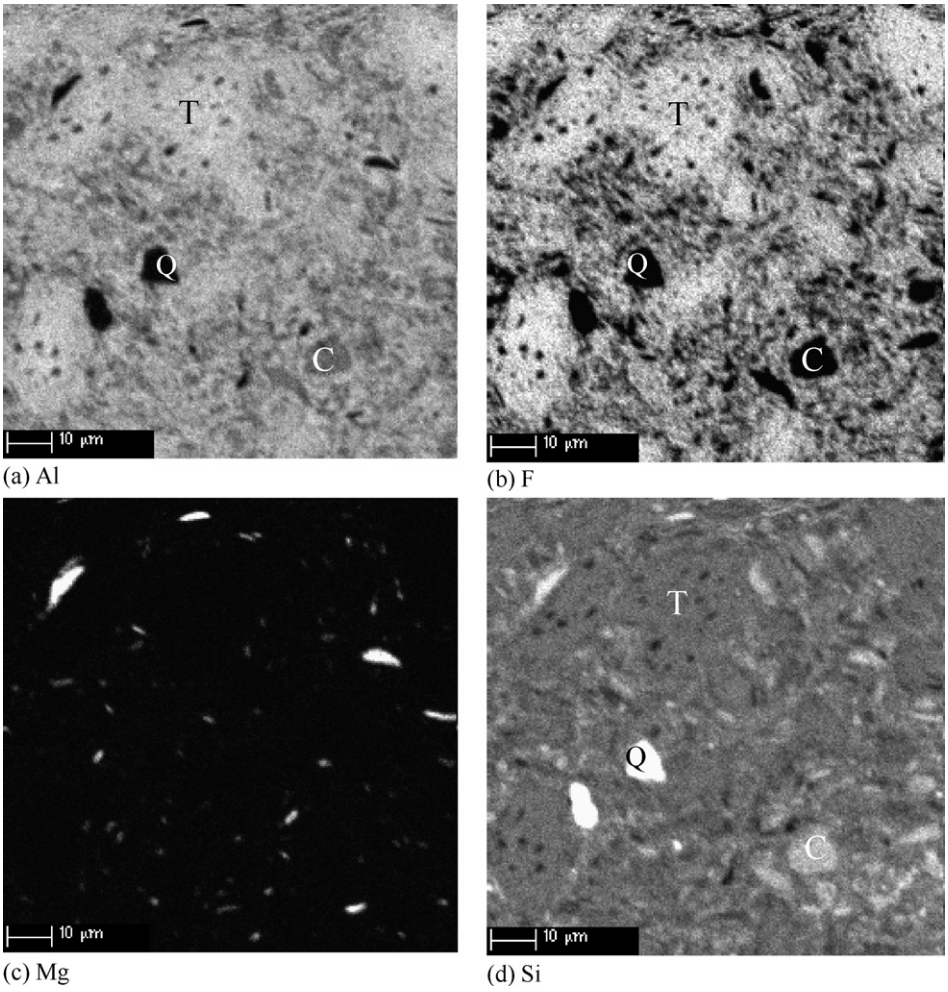

Fig. 2. Element maps of sample from the fluorotopaz phase. T indicates fluorotopaz. C indicates calcined clay. Q indicates quartz.

debindered and calcined at 1100 °C for 1 h. Rectangular samples approximately 4 mm × 9 mm × 50 mm were cut from the calcined honeycomb to conduct experiments on the formation of mullite. One study, referred to as the mechanism study, involved converting the samples to mullite by different paths in temperature and partial pressure of SiF_4. The samples were either reacted in air furnace or in a laboratory quartz reactor in the presence of SiF_4. The temperatures of these reactions were 1100 °C for 30 min (SiF_4 and air) and 1500 °C for 60 min in air.

Another study, referred to as the quenching study, involved converting the samples to mullite in a laboratory quartz tube reactor. For the first stage of the reaction (fluorotopaz formation) the reactor was heated to 800 °C and SiF_4 gas was added at a rate of 2 cm^3/(min g precursor). After the completion of fluorotopaz formation, additional gas was added in order to maintain the partial pressure of SiF_4 in the reactor at 400 mm Hg, and the reactor was heated at 2 °C/min. At about 1050 °C, mullite formation commenced. Since mullite formation is associated with the release of SiF_4, the extent of conversion of fluorotopaz to mullite can be determined by monitoring the SiF_4 gas flow out of the reactor. The reaction was arrested at various degrees of conversion to mullite by rapidly pulling the samples out of the reactor hot zone.

2.2. Characterization of microstructure by SEM and electron microprobe

In some cases samples were fractured, coated with gold–palladium, platinum, or carbon, and examined in either an Amray 1810 scanning electron microscope (SEM) at 15–20 keV,

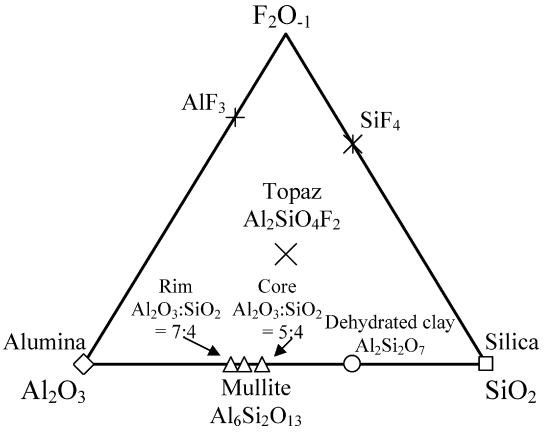

Fig. 3. Chemographic diagram on an atomic basis illustrating the compositions of phases involved in the production of acicular mullite.

an FEI Quanta Inspect SEM at 15 keV, or a JEOL 6320 field emission gun SEM at 5–10 keV. In other cases samples were vacuum-embedded in epoxy, then ground and polished using standard metallographic techniques. Quantitative microanalyses were collected using a Cameca SX50 electron microprobe running SAMx software at 6–10 keV. Element maps were collected with the wavelength dispersive spectrometers (WDS) of the Cameca microprobe at 6–10 keV with some elements acquired using a Ketek silicon drift energy dispersive spectrometer (EDS).

3. Results

3.1. Mechanism of acicular mullite formation

As discussed in Section 1, mullite can be grown into acicular form by two mechanisms, from a melt and through vapor transport. Typically, the presence of fluorine-releasing species is associated with vapor transport[5]; however, the early work of Moyer and Hughes[1] and Moyer and Rudolf[2] and our current results indicate an intimate association with a liquid phase. In order to address this question an experiment was designed where material of the same starting composition was transformed into mullite using three different processing routes. In the first route, mullite precursor was heated in air until full conversion took place, which occurred around 1500 °C (at 1100 °C only about 20% mullite was present). In this approach, direct conversion of a clay and alumina mixture into mullite was accomplished. Neither the 1100 nor 1500 °C sample showed the formation of acicular grains, as illustrated in Fig. 1A and B.

In the second route, the same mullite precursor was heated in flowing nitrogen to 1100 °C. At this temperature SiF_4 was introduced to the system at 500 torr and held for 30 min. According to the fluorotopaz–mullite phase diagram published previously by Moyer,[14] this processing path should lead to the formation of mullite directly from clay and alumina (in the presence of gaseous SiF_4). This sample showed multiple tiny mullite grains growing inside the wall and needles growing on the wall surface (Fig. 1C). The diameter of most of the surface needles was below

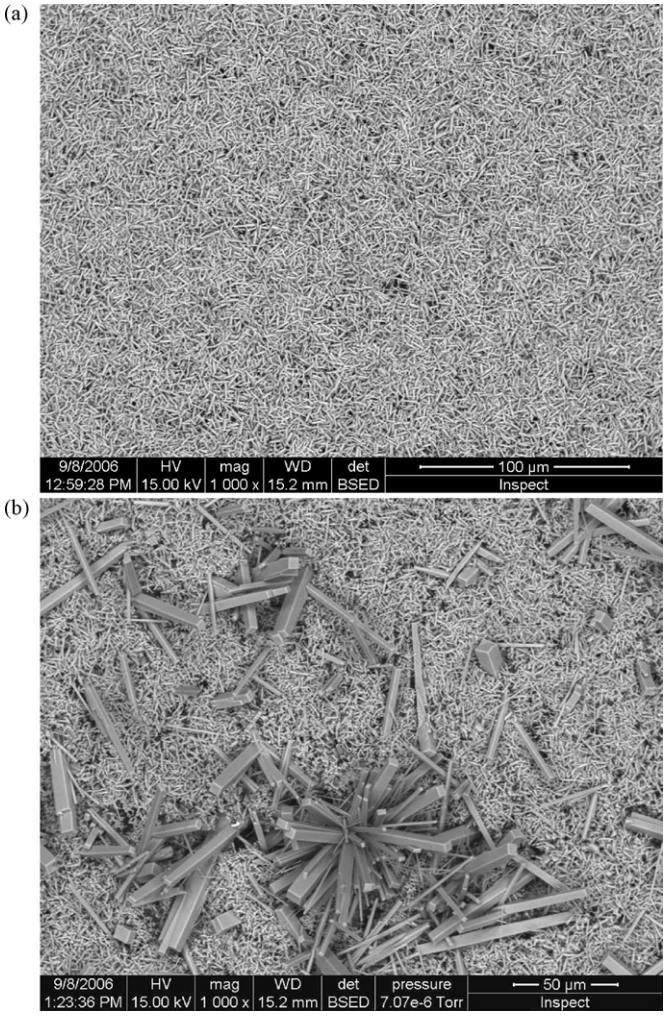

Fig. 4. SEM micrographs of overall microstructure of material (a) just prior to conversion from fluorotopaz to mullite and (b) partially converted from fluorotopaz to mullite.

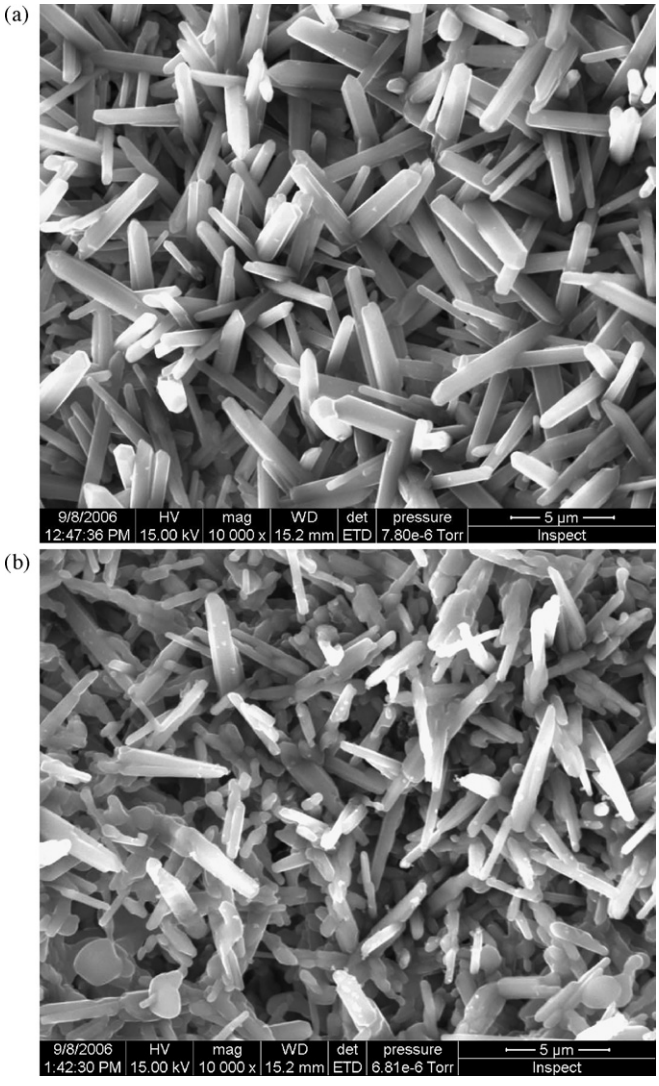

Fig. 5. SEM micrographs of fluorotopaz grains (a) just prior to conversion from fluorotopaz to mullite and (b) a sample that is partially converted from fluorotopaz to mullite.

0.1 μm and aspect ratios were well above 500. We believe they grew through a SiF_4-assisted vapor transport mechanism and that they have a similar appearance to those described in the literature.[11,12] It should be noted, however, that even though the presence of SiF_4 was not very effective in growing large mullite needles it significantly increased the rate of conversion to mullite. While only 20% mullite was produced in the air heated sample, 96% of material was converted to mullite after 30 min in the presence of SiF_4.

The third approach was based on Dow's method for producing mullite by the controlled decomposition of fluorotopaz. In this case, the mixture of alumina and clay was first converted to fluorotopaz which was subsequently pyrolized to form mullite. Similarly to the second approach, mullitization occurred at 1100 °C under a constant pressure of 500 torr SiF_4. However, the difference was that mullitization took place not by directly converting the clay and alumina mixture but by decomposition of fluorotopaz. Crossing the temperature/pressure equilibrium between fluorotopaz and mullite is associated with the formation of a transitional liquid phase (as discussed in later sections) and the growth of large acicular mullite crystals. These crystals can vary in diameter and length depending on process conditions and the starting materials, but they are very different in appearance than those produced by vapor transport such as those in processing route #2. The mullite microstructure produced by decomposition of fluorotopaz via processing route #3 is shown in Fig. 1D. Most of the needles have diameters around 10–15 μm and lengths of 200–300 μm. It is difficult to completely exclude any contribution of vapor transport to mullite growth. But it appears that vapor transport has at best a secondary function and that nucleation and growth of mullite occurs mainly through a liquid phase.

3.2. Mechanism of fluorotopaz to mullite transformation

The mechanism of fluorotopaz to mullite transformation was investigated further by conducting microstructural characterization of samples generated by quenching at different stages of the conversion process. Prior to mullite formation from fluorotopaz some grains of silica and dehydrated clay were still present, along with minor phases containing Ti, Fe, Mg, Ca, and K. The dehydrated clay (metakaolinite) is not likely a stable phase, but persists due to sluggish kinetics. The molecular Al_2O_3:SiO_2 of the calcined clay is 1:2 (the same as kaolinite) as measured by

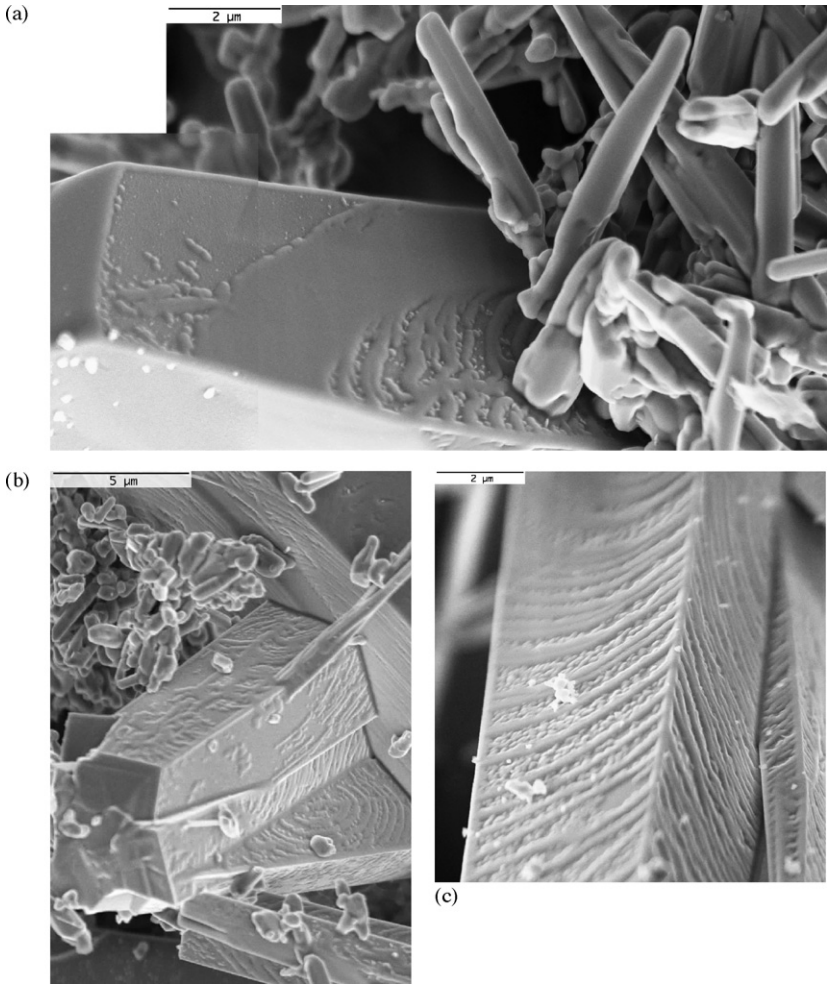

Fig. 6. Sample quenched at partial conversion from fluorotopaz to mullite. (a) Mullite crystal protruding into open space from a channel surface. (b and c) Mullite crystals exposed after fracturing a wall. In all cases, the mullite crystals appeared to be almost completely covered in a glassy phase.

electron microprobe. Bulk X-ray diffraction (XRD) indicated that there was no crystalline phase of this composition, indicating that the metakaolinite was amorphous. Fig. 2 shows element maps of Al, F, Mg, and Si for a sample after conversion of clay plus alumina to fluorotopaz, but before conversion to mullite. Most of the material was composed of small grains of fluorotopaz with small pore spaces between the grains. Dehydrated clay can be recognized by its lack of fluorine and slightly higher silicon and lower aluminum compared to fluorotopaz. Grains of silica and a magnesium silicate can be recognized by their strong silicon and magnesium signals, respectively.

The dehydrated clay reacts away roughly at the same point as the appearance of mullite, suggesting that mullite initially forms via net reactions such as

$$\text{fluorotopaz} + \text{dehydrated clay or silica} = \text{mullite} + SiF_4 \quad (1)$$

$$4Al_2SiO_4F_2 + Al_2Si_2O_7 = 2Al_5Si_2O_{11.5} + 2SiF_4 \quad (2)$$

$$10Al_2SiO_4F_2 + 3SiO_2 = 4Al_5Si_2O_{11.5} + 5SiF_4 \quad (3)$$

The remaining fluorotopaz reacts away via a reaction such as

$$\text{fluorotopaz} = \text{mullite} + \text{alumina} + SiF_4 \quad (4)$$

$$8Al_2SiO_4F_2 = 2Al_5Si_2O_{11.5} + 3Al_2O_3 + 4SiF_4 \quad (5)$$

Alumina is present only transiently, later being incorporated into mullite. The 5:4 composition used for mullite in the equations above is explained in a later section. A chemographic diagram illustrating the compositions of the main phases involved in the conversion of fluorotopaz to mullite is shown in Fig. 3.

The transitional fluorotopaz which forms in the Dow process is in the form of low aspect ratio crystals with typical diameters about 1 μm and a length from 3 to 7 μm. Fig. 4 shows the overall microstructure just before conversion from fluorotopaz to mullite (a), and arrested after partial reaction (b). Once nucleated, mullite crystals grow quickly to most of their final size (10–15 μm × 200–300 μm) before nucleation and growth occurs nearby. The mode of growth is somewhat similar to popcorn. One kernel quickly grows to full size then stops, followed by a grain at a different location quickly growing to full size then stopping. Fig. 5 shows higher magnification micrographs of the fluorotopaz grains in these samples. In the partially reacted sample they appear smaller, rounded and somewhat melted when compared to the unconverted sample. In places, a liquid appears to be present in the partially reacted sample, whereas none is evident in the unconverted sample.

A liquid also appears to coat mullite crystals in the early stages of conversion (Fig. 6). This liquid appears to wet most mullite crystal surfaces and does not pool at concave crystal intersections, indicating a very low surface tension. The presence of this liquid supports, but does not prove, mullite growth from liquid as opposed to vapor. Additional characterization of this glass phase by TEM is ongoing. At later stages of fluorotopaz-to-mullite conversion and in finished parts there is no evidence

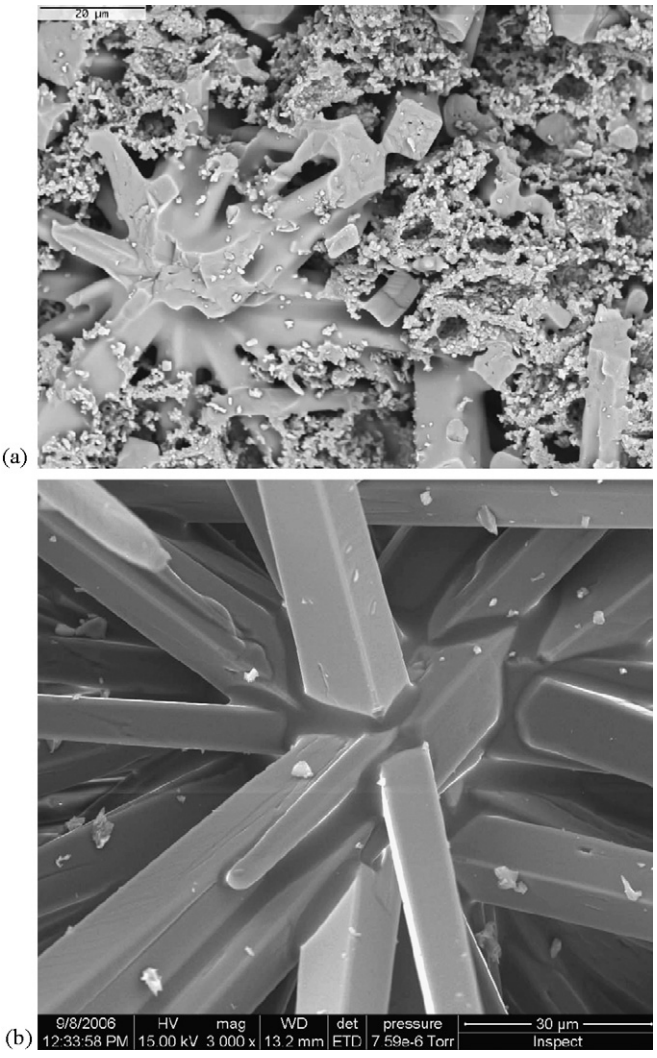

Fig. 7. SEM images of acicular mullite. (a) Fractured partially converted acicular mullite. Small grains are fluorotopaz; large grains are mullite. (b) Typical finished acicular mullite.

for glass coating entire mullite crystals, and the small amount of residual aluminosilicate glass is only present in pools at concave intersections of crystals indicating a much higher surface tension. Analyses of the glass composition in finished parts are reported elsewhere.[13]

Intermediate stages of conversion are characterized by the presence of mullite and fluorotopaz grains in a molten matrix. This is evident in a fractured sample shown in Fig. 7a. The large "starburst" of mullite is surrounded by small fluorotopaz grains in a molten matrix. After the mullitization process continues to completion the final product is acicular mullite. The microstructure formed consists of large mullite grains interpenetrating and intergrown into each other. Additional strength of this network is provided by silica-rich glass which can be observed at mullite grain intersections (Fig. 7b). In finished parts SEM and TEM observation indicate there is no glass coating entire mullite crystals. This geometry indicates a much higher surface tension compared to the melt present in early stages of mullite growth.

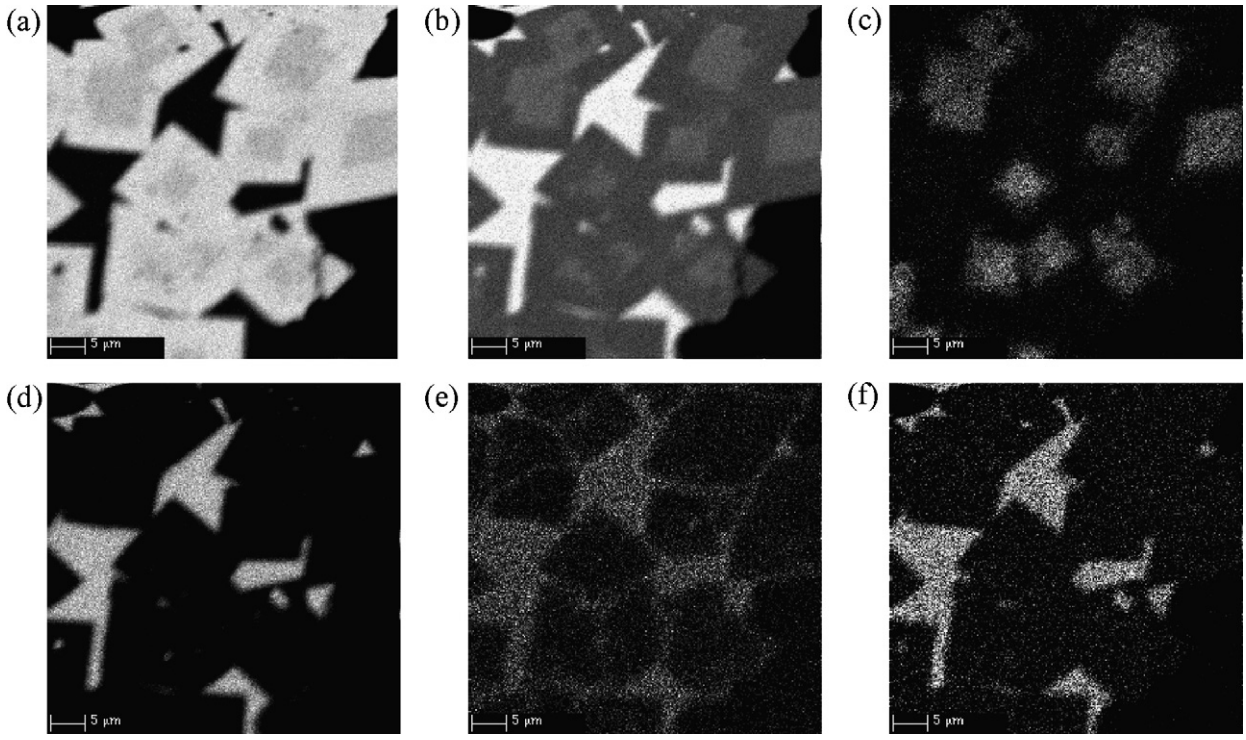

Fig. 8. Element maps of a polished cross-section showing typical elemental zoning of mullite crystals; brightness is a function of weight percent. High-Al grains are mullite; the *c*-axis is oriented roughly perpendicular to the page. The cores of mullite grains have higher Si and Ti compared to the rims. Quantitative microanalyses of mullite are shown in Fig. 9. The high-Si phase between mullite crystals is aluminosilicate glass. Typical finished acicular mullite contains 4–8 vol.% glass. Element maps of: (a) Al; (b) Si; (c) Ti; (d) Mg; (e) Fe; (f) K.

3.3. Composition of mullite

Mullite formed by various solid state and melt-grown reactions has a broad solubility range for alumina.[15] According to the phase diagram developed by Aksay and Pask[16] mullite can contain 69–84 wt.% alumina. However, the exact extent of alumina solubility in mullite is still disputed.[17] Mullite prepared by Moyer and Rudolf[2] by pyrolysis of fluorotopaz had a composition of about 76% Al_2O_3 (as determined by X-ray diffraction from the *a*-lattice parameters). The electron probe analyses conducted in this work shows that the average amount of Al_2O_3 is 66–73%. However, the characterization is complicated by the fact that (i) mullite crystals display elemental zoning and (ii) the ion substitutions into mullite structure are substantial but not identical in the core and at the edge (surface).

Individual mullite crystals commonly display elemental zoning from core to rim. Fig. 8 shows a set of element maps for a cluster of mullite crystals in a pool of glass in a finished acicular mullite sample produced by controlled decomposition of fluorotopaz. The cores have higher Si and Ti whereas the rims have higher Al. The boundary between the two compositions appears quite sharp. This zoning implies that the first mullite formed was Si-rich whereas the mullite grown later was Al-rich. The exact cause of the change in mullite composition during growth is not clear at this time. We hypothesize, however, that it may have to do with resorption of alumina produced during the terminal reaction of fluorotopaz outlined above. A similar phenomenon where small alumina grains dissolved into coexisting silicate glass with subsequent crystallization of higher-alumina mullite was described by Schneider and Komarnei[5] and Schneider and Pleger.[18]

Fig. 9 shows a graph of quantitative microanalyses of mullite crystals from the same sample as in Fig. 8. Microanalyses were normalized to eight cations. The thin solid line represents the solid solution of mullite with no cation impurities. Marks on this line show the location of certain Al_2O_3/SiO_2 molecular and

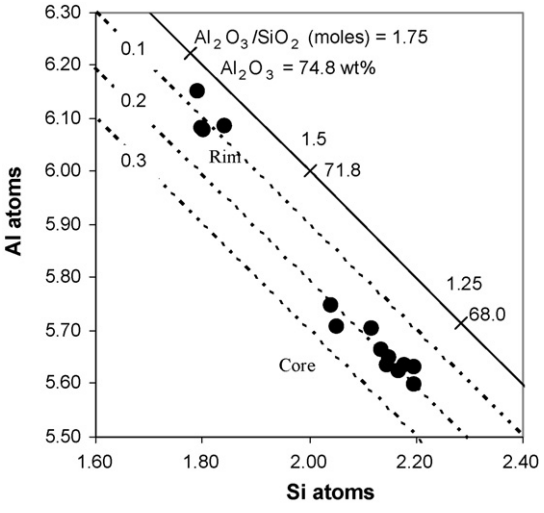

Fig. 9. Quantitative microanalyses of mullite crystals from a standard formulation acicular mullite sample, normalized to eight cations. See text for details.

weight ratios. Typical compositions of acicular mullite produced by fluorotopaz decomposition range from Al_2O_3/SiO_2 molecular ratio ~1.25 (5:4) in the core to ~1.7 in the rim (7:4). This corresponds to 68–74 wt.% Al_2O_3 on an impurity-free basis. These compositions straddle stoichiometric 3:2 mullite. The core is below the 3:2 stoichiometric ratio and has a composition close to the lower limit of alumina solubility predicted by Aksay and Pask's phase diagram. The dashed lines in Fig. 9 represent various levels of cation impurities in mullite from 0.1 to 0.3 atoms (on an eight cation basis). Typical cation impurities measured include Ti, Fe and Mg, and their combined total ranges from around 0.2 atoms in the core to 0.1 in the rim. TiO_2 in this sample ranged from 0.5 up to 3 wt.%. Fe_2O_3 ranged from 1.5 wt.% to below detection. MgO was around 0.5 wt.%. These levels of metallic substitutions are within those reported in the literature.[5] However, their presence further reduces the absolute amount of alumina in the mullite. The interior of mullite crystals can have as little as 66 wt.% Al_2O_3 with the rim around 73 wt.%. This is quite interesting considering that it is a common observation that SiO_2-rich mullite grains tend to be equidimensional and that Al_2O_3-rich mullite tend to have a high aspect ratio.[19]

The intermediate compositions documented here bring up the question of their stability compared to widely cited 3:2 and 2:1 compositions. However, in addition to 3:2 and 2:1 mullite, other compositions such as 3:1[20] and 9:1[21] have been reported to have good chemical stability. Although there are few citations of mullite more Si-rich than 3:2, some exist,[22] and other references cited therein. Recent theoretical calculations also support the stability of alumina-poor compositions.[23] Acicular mullite produced by low temperature and controlled decomposition of fluorotopaz appears to always result in these low-alumina (5:4–7:4) compositions regardless of wide temperature and pressure conditions used. In fact, relatively constant Al_2O_3:SiO_2 ratios were obtained regardless of the Al/Si ratio in the precursor material or the specific type of raw materials used. In addition, when this mullite is heated to 1400 °C it maintains its composition without change in Al/Si ratio. Therefore, the 5:4–7:4 mullite documented in this paper appears to be quite stable.

4. Conclusions

The Dow Chemical Company has developed a ceramic wall flow filter for use as a diesel particulate filter. It is composed of mullite grown from the low temperature (1000–1200 °C) decomposition of fluorotopaz in the presence of silicon tetrafluoride. The unique feature of mullite resulting from this processing route is a highly elongated and well interpenetrated structure of large acicular grains. The acicular mullite grains interlock forming an efficient filter with low back pressure and high mechanical integrity. Porosity remains virtually unchanged until about 1450 °C. Mullite grains have high aspect ratio (~20), and their size can be controlled by raw material and processing variables (diameters chosen from 3 to 50 μm).

Heating precursors in air or introducing SiF_4 at temperature (1100 °C) did not lead to similar mullite microstructures. When heated in air, mullite grains were not acicular. In the second case mullite grew in the form of very small diameter ($\ll$1 μm) high aspect ratio crystals. These very small crystals were similar in appearance to mullite grown by vapor phase transport and reported in the literature.

Characterization of samples quenched during the transformation from fluorotopaz to mullite indicates that growth of mullite was strongly facilitated by a melt. The mullite formed is alumina-poor and chemically zoned from $Al_2O_3/SiO_2 = 1.25$ (molecular) in the core to $Al_2O_3/SiO_2 = 1.7$ in the rim (68–74 wt.% Al_2O_3 on an impurity-free basis).

Impurities (dominated by TiO_2) were higher in the core than in the rim. This 5:4–7:4 mullite appears to be stable under broad temperature conditions.

Acknowledgements

The authors wish to thank Sherry Allen and Tim Gallagher from Core R&D of Dow Chemical Company and Nick Shinkel, Heather Holdaway and Jason Barber from Kelly Scientific in Midland for sample preparation, testing and characterization. The authors also appreciate critical discussions with Dr. John Blackson. Special thanks are due Dr. Cheng Li for his comments and reviewing this manuscript and Dr. Sten Wallin for generating the sample in Fig. 7a of this manuscript.

References

1. Moyer, J. R. and Hughes, N. N., A catalytic process for mullite whiskers. *J. Am. Ceram. Soc.*, 1994, **77**(40), 1083–1086.
2. Moyer, J. R. and Rudolf, P., Stoichiometry of fluorotopaz and mullite made from fluorotopaz. *J. Am. Ceram. Soc.*, 1994, **77**(4), 1087–1089.
3. Pyzik, A. J. and Beaman, D. R., Microstructure and properties of self-reinforced silicon nitride. *J. Am. Ceram. Soc.*, 1993, **76**(11), 2737–2744.
4. Li, C. G., Mao, F., Swartzmiller, S. B., Wallin, S. A. and Ziebarth, R. P., *Properties and Performance of Diesel Particulate Filters of an Advanced Ceramic Material*, SAE Special Publication, 2004-01-0955, 2004.
5. Schneider, H. and Komarneni, S., *Mullite*. Wiley–VCH Verlag GmbH & Co. KGaA, Weinheim, 2005.
6. Perera, D. S. and Allot, G., Mullite morphology in fired kaolinite/halloysite clays. *J. Mater. Lett.*, 1985, **4**, 1270–1272.
7. Li, K., Shimitzu, T. and Igarashi, K., Preparation of short mullite fibers from kaolin via the addition of foaming agents. *J. Am. Ceram. Soc.*, 2001, **84**, 497–503.
8. Hashimoto, S. and Yamaguchi, A., Synthesis of needlelike mullite particles using potassium sulfate flux. *J. Eur. Ceram. Soc.*, 2000, **20**, 397–402.
9. De Sousa, M. F., Regiani, I. and De Sousa, D. P. F., Mullite whiskers from rare earth oxide doped aluminosilicate glasses. *J. Mater. Ceram. Sci.*, 2000, **83**, 60–64.
10. Okada, K. and Otsuka, N., Synthesis of mullite whiskers by vapour-phase reaction. *J. Mater. Sci. Lett.*, 1989, **8**, 1052–1054.
11. Choi, H. J. and Li, J. G., Synthesis of mullite whiskers. *J. Am. Ceram. Soc.*, 2002, **85**, 481–483.
12. Miao, X., Porous mullite ceramics from natural topaz. *Mater. Lett.*, 1999, **38**(3), 167–172.
13. Pyzik, A. J. and Li, C. G., New design of a ceramic filter for diesel emission control application. *Int. J. Appl. Ceram. Technol.*, 2005, **2**(6), 440–451.
14. Moyer, J. R., Phase diagram for mullite–SiF_4. *J. Am. Ceram. Soc.*, 1995, **78**, 3253–3258.
15. Davis, R. F. and Pask, J. A., In *Mullite, in High Temperature Oxides*, ed. A. M. Alper. Academic Press, New York, 1971, pp. 37–76.

16. Aksay, I. A. and Pask, J., Al_2O_3–SiO_2 binary system. *Science*, 1974, **183**(69).
17. Aksay, I. A., Doubbs, D. M. and Sarikaya, M., Mullite for structural, electronic and optical applications. *J. Am. Ceram. Soc.*, 1991, **74**(10), 2343–2358.
18. Schneider, H. and Pleger, R., The reconstructive 2/1 to 3/2 mullite transformation in the presence of Fe_2O_3 rich glass at 1570 °C. *J. Eur. Ceram. Soc.*, 1993, **76**, 2912–2914.
19. Wei, W. and Holloran, J. W., Phase transformations of diphasic aluminosilicate gels. *J. Am. Ceram. Soc.*, 1988, **71**(3), 166–172.
20. Bauer, W. H. and Gordon, I., Flame fusion synthesis of several types of silicate structures. *J. Am. Ceram. Soc.*, 1951, **34**, 250–254.
21. Fisher, R. X., Schneider, H. and Voll, D., Formation of aluminum rich 9:1 mullite and its transformation to low alumina mullite upon heating. *J. Eur. Ceram. Soc.*, 1996, **16**, 109–113.
22. Barta, R. and Barta, C., Study of the system Al_2O_3–SiO_2. *J. Appl. Chem., USSR*, 1956, **29**, 379–389.
23. Mao, H., Selleby, M. and Sundman, B., Phase equilibria and thermodynamics in the Al_2O_3–SiO_2 system—modeling of mullite and liquid. *J. Am. Ceram. Soc.*, 2005, **88**, 2544.